BJP British Journal of Pharmacology

DOI:10.1111/bph.12015
www.brjpharmacol.org

RESEARCH PAPER

Moxifloxacin modifies corneal fibroblast-to-myofibroblast differentiation

TC Chen[1], SW Chang[1,2] and TY Wang[1]

[1]*Department of Ophthalmology, Far Eastern Memorial Hospital, Banqiao District, New Taipei City, Taiwan, and* [2]*Department of Ophthalmology, National Taiwan University Hospital, Taipei, Taiwan*

Correspondence
Dr Shu-Wen Chang, Department of Ophthalmology, National Taiwan University Hospital, 7 Chung-Shan S. Road, Taipei 10002, Taiwan. E-mail: swchang2007@ntu.edu.tw

Keywords
MOX; HCFs; TGFBR1; TGFBR2; fibroblast-to-myofibroblast differentiation; α-SMA filament formation; Smad2 phosphorylation

Received
13 March 2011
Revised
24 September 2012
Accepted
28 September 2012

BACKGROUND AND PURPOSE

Fibroblast-to-myofibroblast differentiation is associated with scarring, an important issue in corneal surgery. Moxifloxacin (MOX), commonly applied to prevent post-operative infection, would benefit more if it modifies fibroblast-to-myofibroblast differentiation other than antimicrobial activity. Our purpose was to explore whether MOX has anti-fibrotic effect in human corneal fibroblasts (HCFs).

EXPERIMENTAL APPROACH

HCFs were incubated in MOX-containing medium concurrently with TGF-β1 (co-treatment), before (pretreatment) or after (post-treatment) adding TGF-β1. HCF contractility was evaluated with a type I collagen gel contraction assay. Expression of α-smooth muscle actin (α-SMA), Smad2, phospho-Smad2-Ser467, Smad4 and Smad7 was determined by immunoblotting. Formation of α-SMA-positive filaments and distribution of active Smad2 were observed under confocal microscopy. Expression of TGF-β receptor types I (TGFBR1) and II (TGFBR2) was assessed with flow cytometry.

KEY RESULTS

MOX did not affect gel contractility or α-SMA filament formation in HCFs without TGF-β1 stimulation. MOX did, however, retard HCF-containing gel contractility and α-SMA filament formation following TGF-β1 stimulation in the pretreatment and co-treatment groups but not in the post-treatment group. MOX blocked the expression of Smad2, phospho-Smad2-Ser467 and TGFBR1 under TGF-β1 incubation. Additionally, MOX enhanced Smad7 expression in TGF-β1-incubated HCFs, but did not interfere with TGF-β-triggered Smad2 nuclear translocation or Smad4 expression.

CONCLUSIONS AND IMPLICATIONS

MOX inhibited TGF-β-induced fibroblast-to-myofibroblast differentiation via blocking TGFBR1 and enhancing Smad7 expression. MOX should be used before or during surgery to achieve these effects. These results suggest a *de novo* mechanism by which MOX participates in corneal wound healing.

Abbreviations

HCFs, human corneal fibroblasts; MOX, moxifloxacin; TGFBR1, TGF-β receptor type I; TGFBR2, TGF-β receptor type II; α-SMA, α-smooth muscle actin

Introduction

Myofibroblasts synthesize and remodel the extracellular matrix during the physiological wound healing process at injured sites (Netto *et al.*, 2005; Hinz *et al.*, 2007). Corneal scarring is characterized by the appearance of corneal myofibroblasts with tissue contraction (Saika *et al.*, 2008), albeit not to the same extent as in other tissues because the cornea is avascular (Saika *et al.*, 2006). TGF-β1, one of the profibrotic TGF-β isoforms in mammals (Tandon *et al.*, 2010), plays an

important role in fibroblast-to-myofibroblast differentiation and in Smad-dependent autocrine TGF-β1-activated signalling, which is crucial for the maintenance of TGF-β1 levels (Webber *et al.*, 2009). Normally, TGF-β1 is present in corneal epithelial and endothelial cells but not in keratocytes (Kaji *et al.*, 2001). TGF-β1 expression does, however, increase in keratocytes after corneal surgery (Kaji *et al.*, 2001; Chang *et al.*, 2008a).

To modulate fibroblast-to-myofibroblast differentiation, TGF-β1 binds to TGF-β receptor type II (TGFBR2), which subsequently activates TGF-β receptor type I (TGFBR1). Activated TGFBR1 phosphorylates and thus activates the downstream effector Smad2 at serine 467 site (Smad2-Ser467), which forms a complex with Smad4 and shuttles into the nucleus (Hutcheon *et al.*, 2005; Matsuzaki, 2011). This nuclear translocation of active Smad2 is directly correlated with α-smooth muscle actin (α-SMA) expression (Petridou *et al.*, 2000). Smad7 is an inhibitory Smad (I-Smad) protein for TGF-β signalling which directly interferes with activation of Smad2 by inhibiting the interaction with TGFBR1 (Fukasawa *et al.*, 2004). In contrast, the addition of TGF-β enhances the functional expression of TGFBR1 in corneal fibroblasts (Maltseva *et al.*, 2001) and dermal fibroblasts (Pannu *et al.*, 2007). Expression of TGFBR1 and TGFBR2 on the cell surface may change the expression and intracellular distribution of downstream proteins, such as α-SMA. Of the TGF-β/Smad signalling transduction molecules, α-SMA is the best characterized indicator of irreversible fibroblast-to-myofibroblast differentiation (Huet *et al.*, 2008; Hindman *et al.*, 2010).

Many approaches for inhibiting TGF-β-mediated corneal scarring are under investigation, among which mitomycin C is the most well known and widely applied. This drug does, however, induce significant cell death (Chang, 2005) and more inflammation (Chou *et al.*, 2007; Chang *et al.*, 2010) and renders the cells more vulnerable to external insults (Chang *et al.*, 2008b) after intraoperative application. There is no available drug capable of effectively treating corneal scarring without causing significant side effects (Tandon *et al.*, 2010).

Moxifloxacin (MOX), one of the fourth-generation fluoroquinolones acting on DNA gyrase and topoisomerase IV (Pestova *et al.*, 2000), is commonly applied prophylactically to prevent post-operative bacterial keratitis following corneal refractive surgery (Burka *et al.*, 2005; Chung *et al.*, 2009). This drug would be even more beneficial if it modifies the fibroblast-to-myofibroblast differentiation pathway in addition to its well-known antimicrobial activity. Our current study was undertaken to examine the effects and probable molecular mechanism of MOX on fibroblast-to-myofibroblast differentiation of normal human corneal fibroblasts (HCFs) by TGF-β1.

Methods

Primary HCF cultivation

Primary HCFs were derived from residual donor corneal rims following penetrating keratoplasty. The corneal epithelium and endothelium were first scraped with a sterile surgical blade. The denuded corneal stroma was subsequently cut into small pieces of 1 × 1 × 1 mm in size and incubated in DMEM (Gibco, Grand Island, NY, USA) containing 10% heat-inactivated FBS (Biological Industries, Kibbutz Beit Haemek, Israel) and 2 mg·mL^{-1} collagenase A (Roche Applied Science, Mannheim, Germany) at 37°C for about 6 h. After washing with antibiotics-free DMEM, the isolated HCFs were seeded in antibiotics-free 10% FBS/DMEM in a humidified atmosphere containing 5% CO_2 at 37°C to expand the number of HCFs for subsequent experiments and used between their fourth and tenth passages.

MOX incubation

To analyse the effect of MOX (VIGAMOX®; Alcon Laboratory Inc., Fort Worth, TX, USA) on HCFs during fibroblast-to-myofibroblast differentiation, 3.0 × 10^5 cells were seeded into a 6 cm culture dish and treated at the following day with 0.1% FBS/DMEM as a serumless culture condition containing 0, 10, 50 or 100 μg·mL^{-1} MOX in the presence or absence of 2 ng·mL^{-1} TGF-β1 (R&D Systems, Minneapolis, MN, USA). The cells were examined at different time points for the following assays.

Collagen gel contraction assay

To examine the effect of MOX on the contraction capacity of HCFs, collagen gel was prepared with PureCor® collagen solution (#5005; Advanced BioMatrix, San Diego, CA, USA), containing about 97% type I collagen with remainder type III collagen, referring to the manufacturer's instruction with minor modification (Tang *et al.*, 2010). Briefly, a final 1 mL of gel mixture of 1.2 mg·mL^{-1} PureCor collagen and 1.0 × 10^5 cells·mL^{-1} was prepared in serumless medium at pH 7.2–7.6 in each well of a 24-well plate. In the groups with TGF-β1 and/or MOX, the collagen mixtures were also mixed with 2 ng·mL^{-1} TGF-β1 and/or 100 μg·mL^{-1} MOX. The collagen gels were incubated at 37°C, and images were captured daily with an AxioCam HRc digital camera (Carl Zeiss, Jena, Germany). The surface area of each gel was calculated, and the differences in the reduction of gel surface area, which represents the contraction capacity of HCFs in the various conditions, were evaluated.

Dot blot assay

To determine the expression of TGF-β1 secretions, 200 μL of condition medium from the treated HCFs in a 6 cm dish was mixed directly with 100 μL of 3 × protein sample buffer (180 mmol·L^{-1} Tris–HCl, pH 6.8, 30% glycerol, 6% SDS, 3.75% β-mercaptoethanol) and 10 μL of each sample was loaded on PVDF membrane (Millipore, Bedford, MA, USA). After blocking non-specific binding with 5% BSA (Sigma Aldrich, St. Louis, MO, USA) in TBST (20 mmol·L^{-1} Tris–HCl, pH 7.5, 500 mmol·L^{-1} NaCl, 0.1% Tween-20) for 1 h, the membranes were incubated at 4°C overnight in 5% BSA-containing TBST with the TGF-β1-specific primary antibody (#5249; 1:1000, rabbit monoclonal; Epitomics, Beverly, MA, USA). The PVDF membranes were then incubated at room temperature with horseradish peroxidase-conjugated anti-rabbit (1:10 000) secondary antibody for 1 h. Finally, the blots were developed with ECL chemiluminescence (Millipore) and analysed with a FUJIFILM LAS-4000 Imaging System (FUJIFILM, Tokyo, Japan).

Immunoblotting

To analyse the protein expression of α-SMA, Smad2, active Smad2, Smad4 and Smad7, the treated HCFs in a 6 cm dish were washed with PBS (137 mmol·L^{-1} NaCl, 2.7 mmol·L^{-1} KCl, 10 mmol·L^{-1} Na_2HPO_4, 2 mmol·L^{-1} KH_2PO_4, pH 7.4) and disrupted in RIPA (150 mmol·L^{-1} NaCl, 1% NP-40, 0.2% SDS, 0.5% sodium deoxycholate, 50 mmol·L^{-1} Tris–HCl, pH 7.4) containing complete EDTA-free protease inhibitor cocktail tablet (Cat. No. 04693132001) and PhosSTOP phosphatase inhibitor cocktail tablet (Cat. No. 04906837001) following the manufacturer's instruction (Roche Applied Science). After protein quantification using a BCA Protein Assay kit (Pierce, Rockford, IL, USA), 3 μg of each sample was separated by 10% SDS-PAGE and transferred to PVDF membranes. After blocking non-specific binding with 5% BSA-containing TBST for 1 h, the membranes were incubated at 4°C overnight in 5% BSA-containing TBST with the appropriate primary antibodies: Smad2 (#3103; 1:1000, mouse monoclonal; Cell Signalling Technology, Beverly, MA, USA), phospho-Smad2-Ser467 (sc-101801; 1:1000, rabbit polyclonal; Santa Cruz Biotechnology, Santa Cruz, CA, USA), Smad4 (sc-7154; 1:1000, rabbit polyclonal; Santa Cruz Biotechnology), Smad7 (#3894-1; 1:1000, rabbit monoclonal; Epitomics), α-SMA (A2547; 1:1000, mouse monoclonal; Sigma Aldrich) and β-actin (A5441; 1:1000, mouse monoclonal; Sigma Aldrich). The PVDF membranes were then incubated at room temperature with horseradish peroxidase-conjugated anti-mouse (1:10 000) or anti-rabbit (1:10 000) secondary antibodies for 1 h. Finally, the blots were developed and analysed as described in the 'Dot blot assay'.

To verify if MOX's effect on human corneal fibrosis could be generalized to other fluoroquinolones, we also investigated α-SMA and Smad2 expressions in HCFs after treatment with ciprofloxacin (CIP; Ciproxin®; Bayer Schering Pharma, Leverkusen AG, Germany) and levofloxacin (LEV; CRAVIT®; Sanofi-Aventis Deutschland GmbH, Frankfurt am Main, Germany) in conditions similar to MOX incubation.

Immunofluorescence staining

To observe α-SMA filament formation and intracellular distribution of Smad2, 1.0×10^4 cells were seeded on 12 mm round uncoated cover glasses placed in the wells of a 24-well culture plate and treated at the following day. The cells at the harvested time were fixed with ice-cold 4% paraformaldehyde in PBS for 10 min. After washing with PBS, the fixed cells were incubated in permeabilization blocking solution (0.1% Triton X-100 and 10 mg·mL^{-1} BSA in PBS) for 30 min. The cells were subsequently incubated with appropriate primary antibodies specific for α-SMA (A2547; 1:100; Sigma Aldrich), Smad2 (#3103; 1:100; Cell Signalling Technology) or phospho-Smad2-Ser467 (sc-101801; 1:100; Santa Cruz Biotechnology) for 1 h. After washing twice with PBS, the cells were incubated with Alexa Fluor® 488- or 594-conjugated secondary antibody (1:200; Invitrogen, Carlsbad, CA, USA) in the dark for 1 h. The actin filaments and nuclei were stained with rhodamine phalloidin (Invitrogen) for 30 min and DAPI for 15 min respectively. Finally, the cover glasses were mounted reversely on glass slides with aqueous mounting medium (DAKO, Carpinteria, CA, USA) and analysed with a Zeiss LSM510 confocal system (Carl Zeiss).

To verify if MOX's suppression on α-SMA filament formation could be generalized to other fluoroquinolones, we also observed α-SMA filament formation in HCFs after treatment with CIP and LEV in conditions similar to MOX incubation.

Flow cytometry

To analyse the amount of TGFBR1 and TGFBR2 on the HCF surface, the treated cells in a 6 cm dish were harvested 3 days post incubation with MOX- and/or TGF-β1-containing serumless DMEM, detached with trypsinization, washed three times with PBS, and fixed with ice-cold 4% paraformaldehyde in PBS for 10 min. After washing with PBS, the fixed cells were blocked for 30 min in non-permeabilization blocking solution (10 mg·mL^{-1} BSA in PBS). They were then incubated with primary antibodies, TGFBR1 (sc-33933; 1:100; goat polyclonal; Santa Cruz Biotechnology) and TGFBR2 (sc-17791; 1:100; mouse monoclonal; Santa Cruz Biotechnology), for 1 h, washed three times with PBS, and labelled with Alexa Fluor 488-conjugated anti-goat and anti-mouse secondary antibodies for 1 h respectively. Fluorescence intensity of the labelled HCFs was detected by BD FACSCalibur and analysed by WinMDI software (BD Biosciences, San Jose, CA, USA).

Statistical analysis

All the experiments were performed independently in triplicate and the data were analysed by SPSS® version 16 software (SPSS Inc., Chicago, IL, USA). The data were analysed by one-way or two-way ANOVA followed by Tukey's honestly significant difference *post hoc* test for multiple comparisons. The *P*-value of less than 0.05 was considered statistically significant.

Results

Reduction of TGF-β1-induced gel contraction

MOX alone did not alter collagen gel size in the absence of TGF-β1 (Figure 1, well 2). Addition of TGF-β1 to the medium resulted in a 30% reduction in the collagen gel surface area (Figure 1, well 3). MOX noticeably reversed the contraction capacity of HCF-containing gel in the presence of TGF-β1, that is, only 10% reduction in collagen gel surface area was observed (Figure 1, well 4). This suggests that MOX is potentially beneficial in preventing fibrotic contraction.

Induction of TGF-β1 secretions

To determine the amount of TGF-β1 in the condition medium of the treated HCFs in the absence or presence of recombinant TGF-β1, we used dot blot assay to determine the TGF-β1 expression at several time points (Figure 2). The results revealed that TGF-β1 alone triggered secretory TGF-β1 expression time-dependently, especially at 48 and 72 h. This suggests that TGF-β1 stimulation acted in an autocrine regulation manner to enhance TGF-β1 secretion in HCFs. In the presence of MOX, the related late TGF-β1 surge was abolished.

Suppression of newly synthesized α-SMA expression

MOX alone did not modify intracellular α-SMA protein expression (Figure 3, lanes 2–4). MOX did, however, suppress

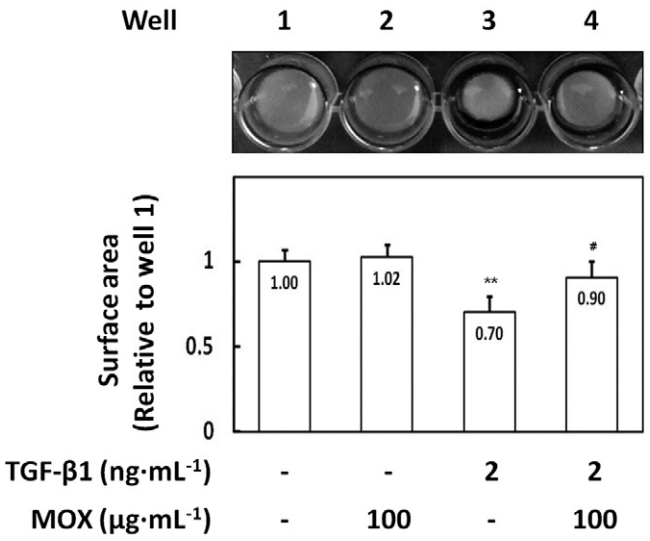

Figure 1

MOX reduction of HCF-containing gel contractility. HCFs were mixed with PureCor collagen solution as shown below the graph. Images were captured after co-incubation of 100 μg·mL^{-1} MOX and/or 2 ng·mL^{-1} TGF-β1 for 3 days. Quantitative data were expressed as the mean ± SEM of four individual experiments performed in triplicate. Differences in the relative change of surface area were analysed by one-way ANOVA and compared with the groups in the absence of TGF-β1 (**, $P < 0.01$) or MOX (#, $P < 0.05$).

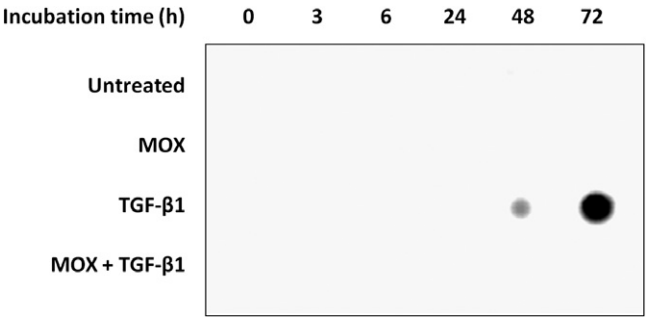

Figure 2

Up-regulation of TGF-β1 secretions in TGF-β1-stimulated HCFs. HCFs were incubated in 2 ng·mL^{-1} TGF-β1-containing serumless DMEM with 100 μg·mL^{-1} MOX, and the condition medium was harvested at 0, 3, 6, 24, 48 and 72 h. All the condition samples were analysed by dot blot assay with TGF-β1-specific antibody. This was performed in triplicate with similar trend for TGF-β1 expressions.

α-SMA expression in a dose-dependent manner when it was co-incubated with TGF-β1 (co-treatment; Figure 3, lanes 6–8).

To further assess the most appropriate time for MOX application to suppress TGF-β1-enhanced α-SMA expression, we incubated HCFs in MOX-containing serumless culture medium before (pretreatment; Figure 4A) or after TGF-β1 incubation (post-treatment; Figure 4B). Immunoblotting revealed that pretreatment with MOX for 1 day significantly inhibited α-SMA expression in HCFs in the presence of TGF-β1 (Figure 4A, lanes 7 and 8). However, when the cells were treated first with TGF-β1 for 1 day (Figure 4B), MOX could not modify the already-expressed α-SMA. These results suggest that MOX application following TGF-β1 treatment provided no additional suppression of TGF-β1-induced α-SMA expression.

Inhibition of TGF-β1-induced α-SMA filament formation

Immunofluorescence staining revealed no α-SMA filaments in untreated cells (Figure 5A) and in MOX-treated fibroblasts (Figure 5D), whereas incubation with TGF-β1 significantly increased α-SMA filament formation (Figure 5G). MOX treatment significantly decreased incorporation of α-SMA into filaments in TGF-β1-incubation fibroblasts (Figure 5J). MOX efficiently reduced the α-SMA filament formation from 30.8% (12.5% strong plus 18.3% weak) to 1.7% (0.4% strong plus 1.3% weak) in TGF-β1-treated cells (Figure 5M) in addition to suppressing endogenous α-SMA expression *per se*. These morphological observations confirmed that MOX inhibited corneal fibroblast-to-myofibroblast differentiation.

Blockage of TGFBR1 expression on the fibroblast surface

To examine whether MOX exerted its effect via modifying TGF-β receptor complex expression on the cell surface, we determined the signal intensity of green fluorescent dye-labelled TGFBR1 (Figure 6A) and TGFBR2 (Figure 6B) using flow cytometry. The results disclosed that MOX alone did not modify the number of TGFBR1- and TGFBR2–labelled HCFs (Figure 6A and B, blue curve). Addition of recombinant TGF-β1 resulted in a significant increase in TGFBR1-labelled HCFs (Figure 6A, red curve), but did not change the expression of TGFBR2 (Figure 6B, red curve). In contrast, MOX co-treatment abolished the TGF-β1-related right shift of the curve (Figure 6A, green curve). These data indicate that blockage of the TGFBR1, but not TGFBR2, response to TGF-β1 stimulation might be a key factor for MOX-related suppression of corneal fibrosis in HCFs.

Alteration of protein expression and phosphorylation of Smad2

To verify the role of MOX in Smad2/Smad4 complex-related corneal fibrosis, we determined the levels of Smad2, Smad4, Smad7 and active Smad2 after MOX incubation (Figure 7). Immunoblotting showed that MOX had no noticeable effect on expression of phospho-Smad2-Ser467, Smad2, Smad4 and Smad7 in the absence of TGF-β1. However, MOX did noticeably reduce the expressions of both TGF-β1-activated Smad2 (Figure 7A and B, lanes 16–20) and endogenous Smad2 (Figure 7A and C, lanes 16–20) in a time-dependent manner under TGF-β1 stimulation. MOX did not modulate Smad4 expression (Figure 7A and D). Nevertheless, MOX time-dependently induced Smad7 expression (Figure 7A and E, lanes 16–20), also only in the presence of TGF-β1 stimulation. Thus, MOX might benefit fibrosis prevention by enhancing Smad7 expression, which subsequently suppressed Smad2 synthesis and phosphorylation during wound healing.

No effect on nuclear translocation of Smad2

Due to the importance of nuclear translocation of active Smad2 on fibroblast-to-myofibroblast differentiation during

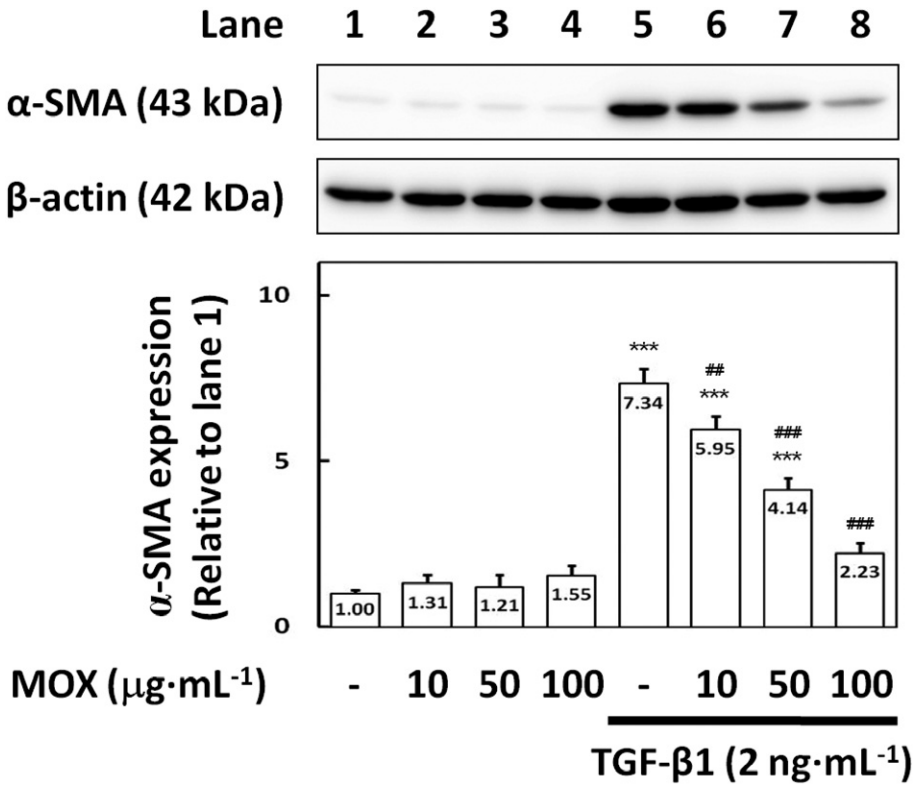

Figure 3

MOX suppression of α-SMA expression. HCFs were incubated in 2 ng·mL^{-1} TGF-β1-containing serumless DMEM with 0, 10, 50 or 100 μg·mL^{-1} MOX. Cells were harvested after 3 days of incubation and analysed by immunoblotting with α-SMA- and β-actin-specific primary antibodies. Quantitative data were expressed as the mean ± SEM of three individual experiments performed in triplicate. Differences in the relative change of α-SMA expression were analysed by two-way ANOVA and compared with the groups in the absence of TGF-β1 (***, $P < 0.001$) or MOX (##, $P < 0.01$; ###, $P < 0.001$).

wound healing, we used immunofluorescent staining to monitor the distribution of Smad2 and phospho-Smad2 (Figure 8). Endogenous Smad2 in the untreated HCFs was scattered mainly in the cytoplasm (Figure 8A), but active Smad2 was undetectable in the entire cell (Figure 8B). MOX alone did not alter the staining pattern of Smad2/active Smad2 in cells (Figure 8D and E). TGF-β1 induced nuclear translocation of Smad2/active Smad2 (Figure 8G, H and I). Smad2/Active Smad2 could still shuttle into the nucleus of MOX-treated HCFs in the presence of TGF-β1 (Figure 8J, K and L). These results indicate that MOX did not interfere with the TGF-β1-induced intracellular shuttling of active Smad2 in HCFs.

Anti-fibrotic efficiency of other fluoroquinolones in HCFs

In addition to MOX, the fibrosis-suppressing effect of two other fluoroquinolones, CIP (a second-generation agent) and LEV (a third-generation agent), was examined (Figure 9). The immunoblotting revealed that CIP or LEV alone did not noticeably modify intracellular protein expression of α-SMA (Figure 9C and D, lanes 2–4) and Smad2 (Figure 9E and F, lanes 2–4). However, both CIP and LEV suppressed TGF-β1-stimulated α-SMA expression (Figure 9C and D, lanes 6–8) and TGF-β1-incubated Smad2 expression in a dose-dependent manner (Figure 9E and F, lanes 6–8). Immunofluorescence staining also revealed that CIP and LEV were able to reduce the TGF-β1-related α-SMA filament formation cells from 30.8% (12.5% strong plus 18.3% weak) to residual 5.1% (0.6% strong plus 4.5% weak) and 9.8% (2.7% strong plus 7.1% weak) respectively (Figure 10). Statistical analysis revealed that CIP and LEV also manifested anti-fibrotic effect as did MOX, but not as efficiently ($P < 0.001$).

Discussion and conclusions

Minimized post-operative scar formation and the absence of infection are prerequisites for perfect refractive surgery results. In this study, we investigated the inhibitory effect of MOX on fibroblast-to-myofibroblast differentiation in the presence of TGF-β1, a scenario mimicking wound healing. We demonstrated for the first time that MOX at concentration of 100 μg·mL^{-1}, a non-lethal dose in HCFs, was sufficient to reduce HCF-containing gel contractility (Figure 1), endogenous α-SMA filament formation (Figure 5) and TGFBR1 expression on the HCF surface (Figure 6A), suggesting that MOX may reduce fibroblast-to-myofibroblast differentiation in human corneal stroma.

Our results revealed that both co-treatment (Figure 3) and pretreatment (Figure 4A) with MOX efficiently reduced

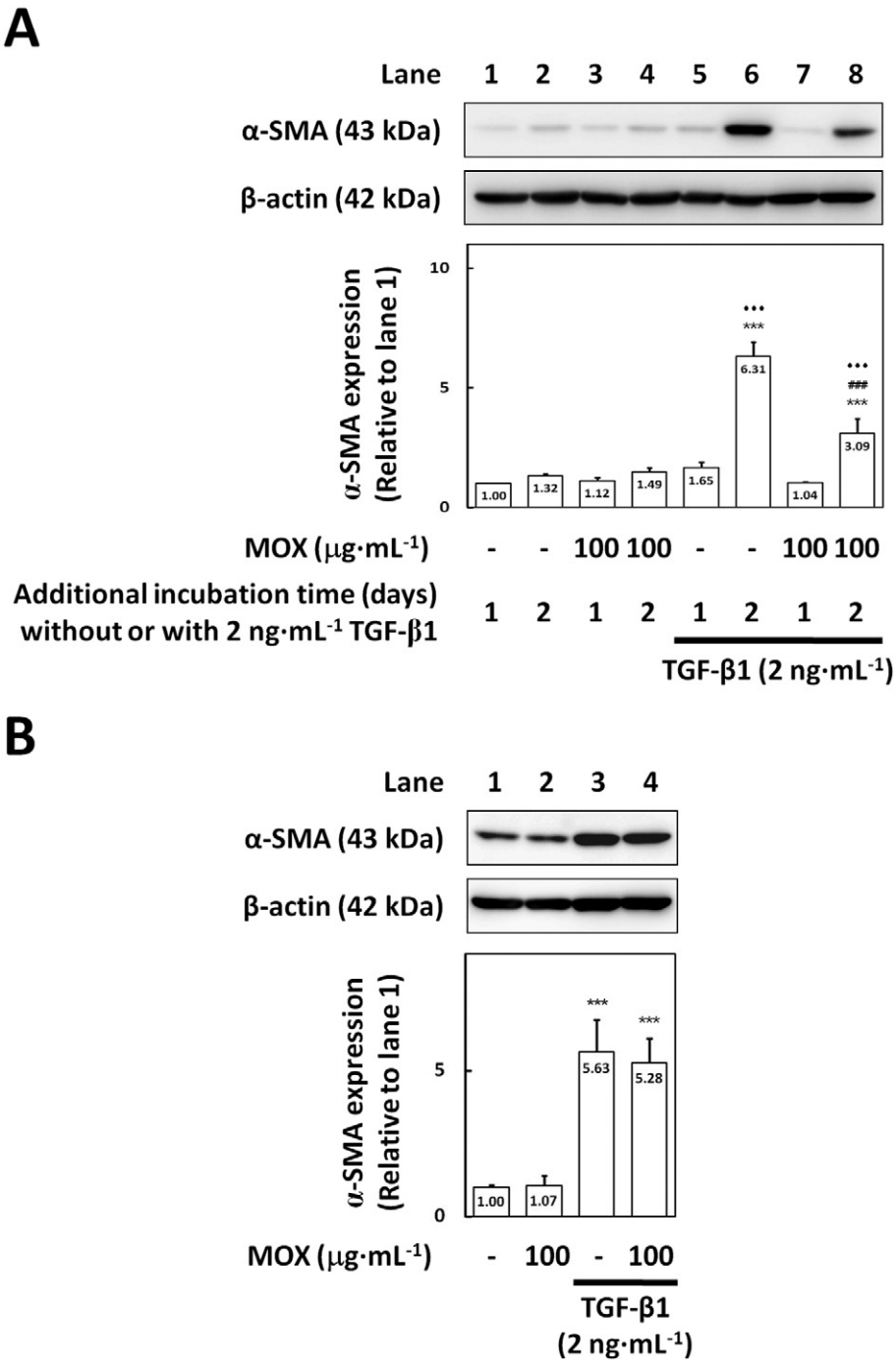

Figure 4

Suppression efficiency of MOX on α-SMA expression. (A) HCFs were untreated (lanes 1, 2, 5 and 6) or pretreated with (lanes 3, 4, 7 and 8) 100 μg·mL^{-1} MOX for 1 day and then incubated in serumless DMEM without (lanes 1–4) or with (lanes 5–8) 2 ng·mL^{-1} TGF-β1 for a further day. Additional incubation time (days): the number of days incubated in TGF-β1-containing media after pretreatment with MOX. (B) HCFs were treated in serumless DMEM with 2 ng·mL^{-1} TGF-β1 for 1 day before co-incubating with 100 μg·mL^{-1} MOX for 1 more day. The cell lysates were harvested at 2 day TGF-β1 stimulation and analysed by immunoblotting with α-SMA- and β-actin-specific primary antibodies. Quantitative data were expressed as the mean ± SEM of three individual experiments performed in triplicate. Differences in the relative changes of α-SMA expression were analysed by two-way ANOVA for (A) or one-way ANOVA for (B), and compared with the groups in the absence of TGF-β1 (***, $P < 0.001$) or MOX (###, $P < 0.001$) at the same harvest day, and also compared with the same treatment groups at the previous day (◆◆◆, $P < 0.001$).

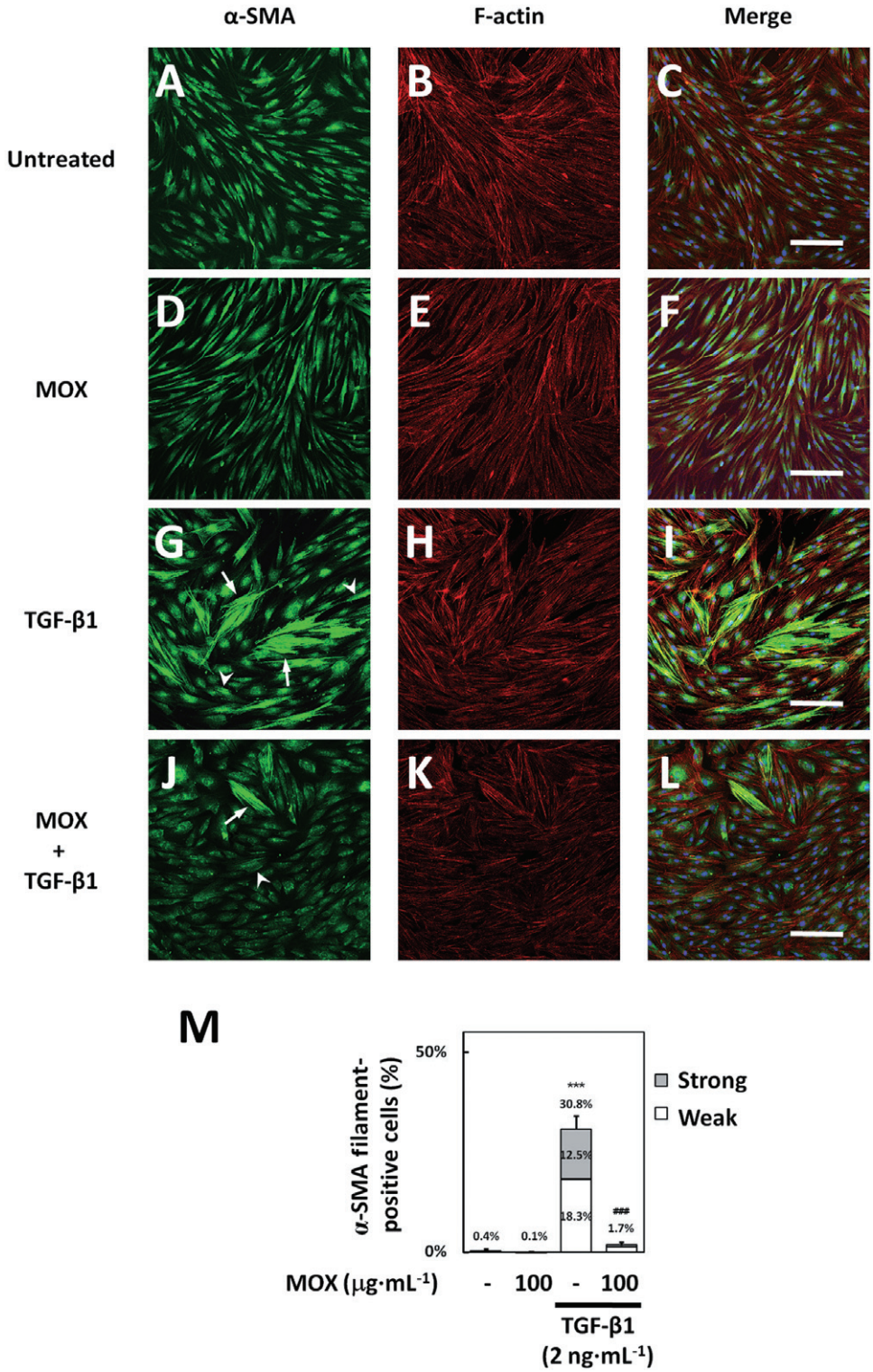

Figure 5

MOX suppression of α-SMA filament formation. HCFs on round cover glasses were with 100 μg·mL^{-1} MOX and/or 2 ng·mL^{-1} TGF-β1 for 3 days and then were stained with α-SMA-specific antibody (A, D, G, J), rhodamine phalloidin (B, E, H, K) and DAPI (shown in merged images C, F, I, L). Scale bar in each merged image was 100 μm in length. (M) Ratio of α-SMA filament-positive cells was calculated as cells stained both strongly (arrows, upper part of the column) and weakly (arrowheads, lower part of the column) for α-SMA filament divided by all visualized cells from five different fields of each individual experiment at 100 × magnification. The total expression ratios were expressed as the mean ± SEM of three individual experiments performed in triplicate. Differences in the relative ratios were analysed by one-way ANOVA and compared with the groups in the absence of TGF-β1 (***, $P < 0.001$) or MOX (###, $P < 0.001$).

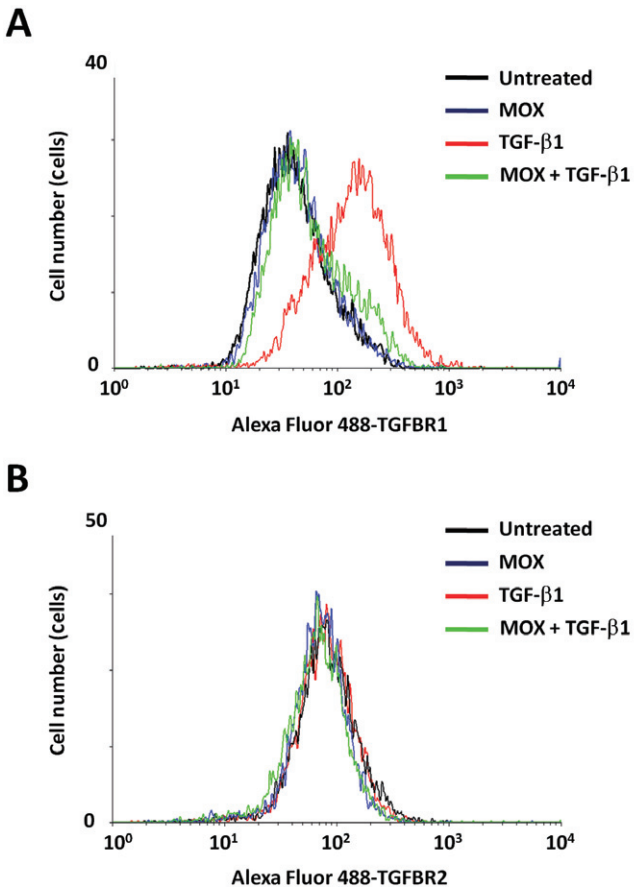

Figure 6

MOX down-regulation of TGFBR1 expression on the surface of HCFs. HCFs were co-incubated with 100 μg·mL^{-1} MOX and/or 2 ng·mL^{-1} TGF-β1 for 3 days. Cells were incubated with (A) TGFBR1- and (B) TGFBR2-specific antibodies, stained with fluorescent Alexa Fluor 488-conjugated anti-goat and anti-mouse secondary antibodies, respectively, and analysed with flow cytometry. Displayed curve represents one of the individual experiments performed in triplicate for TGFBR1 and TGFBR2 expressions respectively.

TGF-β1-related α-SMA production, but MOX treatment after TGF-β1 incubation did not dissipate the already-formed α-SMA (Figure 4B). These results are consistent with a previous report that TGF-β1 induced a relatively stable fibroblast phenotype alteration in myofibroblasts (Evans *et al.*, 2003). As TGF-β1 increases in an autocrine augmentation manner both *in vivo* (Kaji *et al.*, 2001) and *in vitro* (Kato *et al.*, 2011), the sustained up-regulation of TGF-β1 secretion (Figure 2) might be critical in more α-SMA filament formation (Figure 5), more TGFBR1 expression on cell surface (Figure 6) and the observed long-term Smad2 activation (Figure 7B). Therefore, we suggest that MOX should be applied before corneal fibroblasts differentiate into corneal myofibroblasts. Clinically, MOX is commonly used post-operatively (Holland *et al.*, 2008), although some surgeons advocate preoperative administration for better antimicrobial prophylaxis (Katz *et al.*, 2005; Holland *et al.*, 2008; Yoshida *et al.*, 2010). We suggest that application of MOX before surgery is more beneficial in terms of fibroblast-to-myofibroblast differentiation and subsequent wound healing.

MOX blocked TGF-β1 from increasing TGFBR1 on corneal fibroblasts (Figure 6A), but had no obvious effect on TGFBR2 expression (Figure 6B). However, MOX induced Smad7 expression in TGF-β1-incubated HCFs (Figure 7A and E), suggesting that the increased Smad7 might inhibit the interaction between TGFBR1 and Smad2. Furthermore, TGFBR1 controls the TGF-β signalling pathway (Blobe *et al.*, 2000), so we propose that blocking the TGFBR1 expression in response to TGF-β exposure may be the critical mechanism for how MOX suppresses TGFBR1 signalling-related α-SMA filament formation. MOX also noticeably attenuated Smad2 phosphorylation (Figure 7A and B) and TGF-β1-stimulated Smad2 protein expression (Figure 7A and C). It did not, however, affect TGF-β1-triggered nuclear translocation of active Smad2 in HCFs (Figure 8). Nuclear translocation of active Smad2/Smad4 complexes is a key step during TGF-β1-triggered differentiation of myofibroblasts (Blobe *et al.*, 2000). In addition, Smad2 phosphorylation is required during fibroblast-to-myofibroblast differentiation (Petridou *et al.*, 2000), and Smad2 overexpression results in up-regulation of α-SMA transcripts in fibroblasts (Evans *et al.*, 2003). Therefore, we believe that the MOX-related decrease in α-SMA filament formation resulted from reduced protein expression and phosphorylation of endogenous Smad2.

We demonstrated that MOX modified α-SMA expression and fibroblast-to-myofibroblast differentiation by modifying TGF-β1 signalling. This mechanism is different from that of the widely used mitomycin C, which modulates wound healing mainly by inducing keratocyte apoptosis (Chang, 2005). MOX is thus a potential candidate for facilitating corneal wound healing without inducing excessive keratocyte loss and is thus devoid of this potential long-term concern.

Medications could be applied at different dosages for different purposes. For example, oral cimetidine facilitates the healing of benign gastric ulcer at a dosage of 300 mg with meals and at bedtime (Isenberg *et al.*, 1983). At higher dosage, it results in augmentation of both cellular and humoral immunity and has been used clinically for papillomatosis treatment (Chang and Huang, 2006). Similarly, the minimum concentration of MOX needed to inhibit 90% of pathogens commonly encountered is in the range of 0.25–2.5 μg·mL^{-1} (Kernt *et al.*, 2009). Higher stromal concentration of 48.5 μg·g^{-1} could be achieved by topical application of 5 mg·mL^{-1} MOX 2 doses given 5 min apart (Holland *et al.*, 2008), and no significant toxicity of MOX is observed on human corneal endothelium with concentrations up to 150 μg·mL^{-1} (Kernt *et al.*, 2009). In this study, we demonstrated that MOX exerted anti-fibrotic effects on HCFs at higher doses of 50–100 μg·mL^{-1} (Figures 3 and 5). Because higher tissue level could be achieved by adding retention-enhancing agent in the formula (Lindstrom *et al.*, 2010), careful dosage adjustment could thus provide reasonable antimicrobial and anti-fibrotic effects. Furthermore, as corneal epithelium is a critical barrier to topically applied medication (Yasueda *et al.*, 2007), corneal penetration of topically applied antibiotics would increase tremendously in cases with corneal epithelial defects, such as corneal ulcers. We suggest that stromal concentration of higher than 100 μg·mL^{-1} could be achieved by topical frequent application of 5 mg·mL^{-1} MOX in these cases. As corneal scar formation following corneal ulcer usually leads to corneal

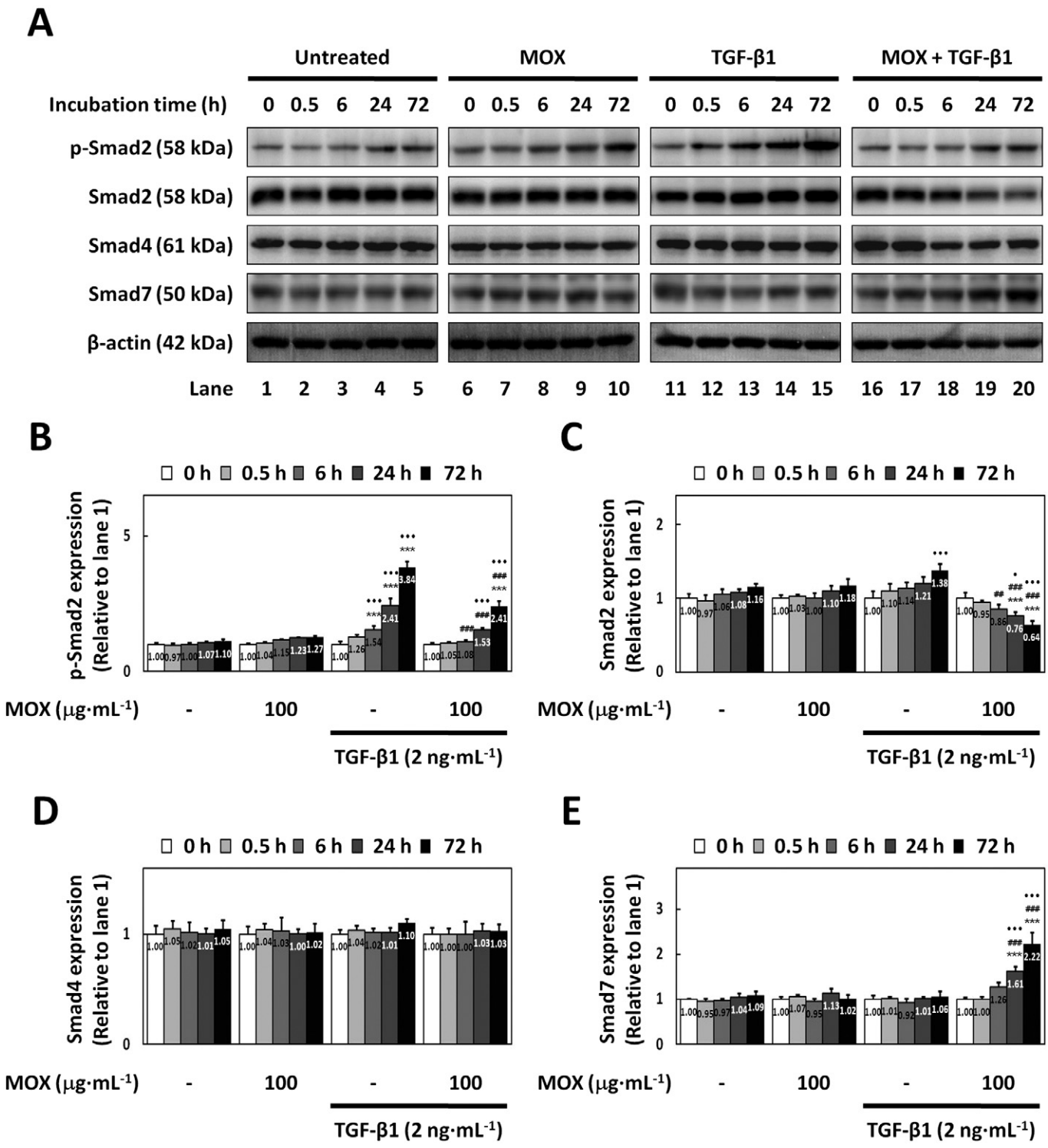

Figure 7

MOX inactivation of Smad2 expression. HCFs were incubated in 2 ng·mL^{-1} TGF-β1-containing serumless DMEM with 0 or 100 μg·mL^{-1} MOX. (A) Cells were harvested at the incubation time points and analysed by immunoblotting with phospho-Smad2-Ser467 (p-Smad2)-, Smad2-, Smad4-, Smad7- and β-actin-specific primary antibodies. (B) Relative p-Smad2 expression was calculated and normalized to the present endogenous Smad2. Relative expressions of (C) Smad2, (D) Smad4 and (E) Smad7 were calculated and normalized to β-actin expression respectively. Quantitative data were expressed as the mean ± SEM of three individual experiments performed in triplicate. Differences in the relative changes of p-Smad2, Smad2, Smad4 and Smad7 expressions were analysed by two-way ANOVA compared with the groups in the absence of TGF-β1 (***, $P < 0.001$) or MOX (##, $P < 0.01$; ###, $P < 0.001$), and also compared with the same treatment groups at 0 h (◆, $P < 0.05$; ◆◆◆, $P < 0.001$).

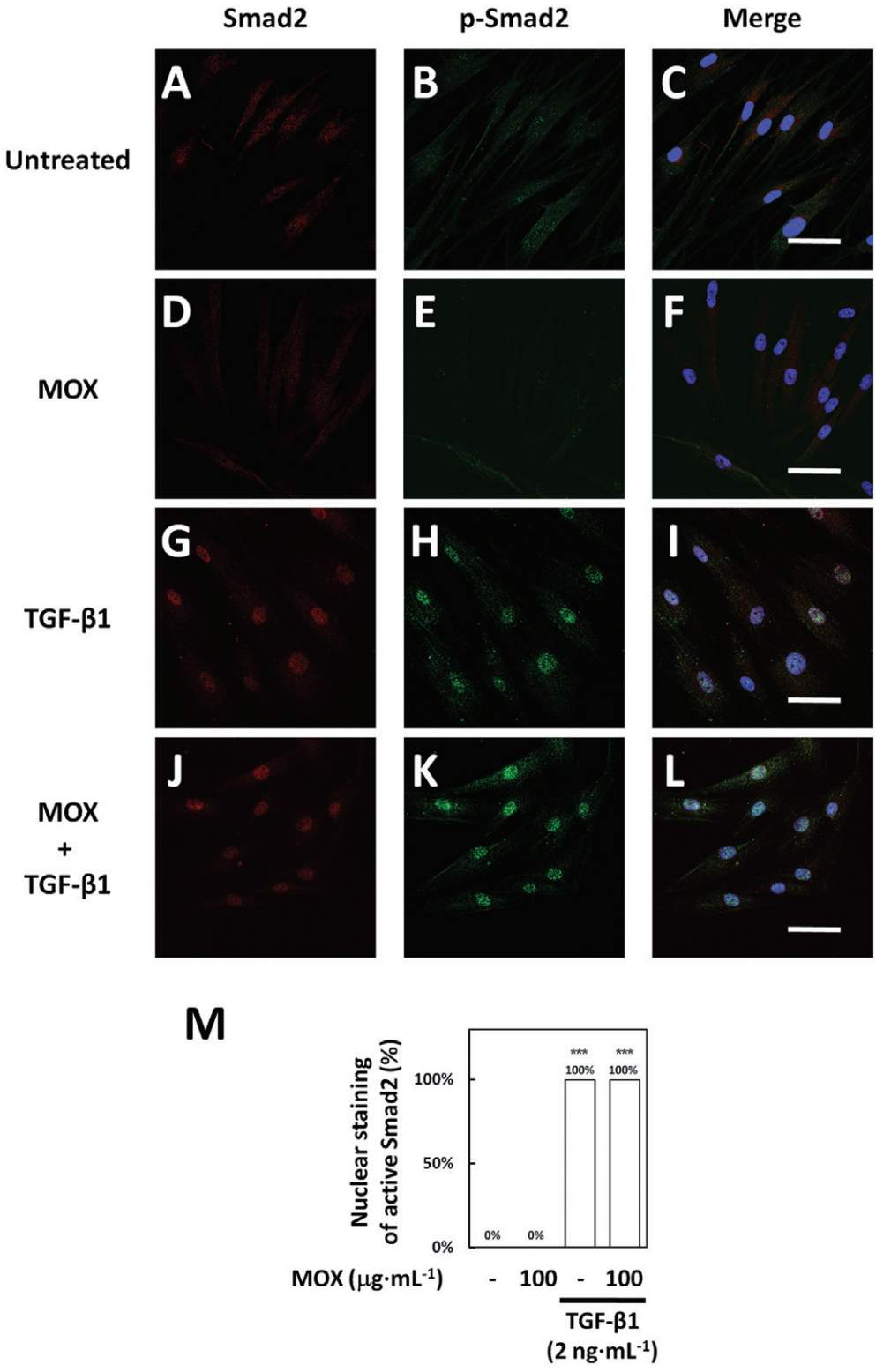

Figure 8

No change in Smad2 nuclear shuttling by MOX. HCFs on round cover glasses were co-incubated with 100 μg·mL^{-1} MOX and/or 2 ng·mL^{-1} TGF-β1 for 3 days and stained with anti-Smad2 (A, D, G, J), anti-phospho-Smad2-Ser467 (p-Smad2) (B, E, H, K) and DAPI (shown in merged images of C, F, I, L). These confocal images were captured from the fields at 400 × magnification. Scale bar in each merged image was 50 μm in length. (M) Ratio of active Smad2 in nucleus was calculated from five different fields of each individual experiment at 400 × magnification. Quantitative data of total expression ratio were expressed as the mean ± SEM of three individual experiments performed in triplicate. Differences in the relative changes of active Smad2 in nucleus were analysed by one-way ANOVA and compared with the groups in the absence of TGF-β1 (***, $P < 0.001$).

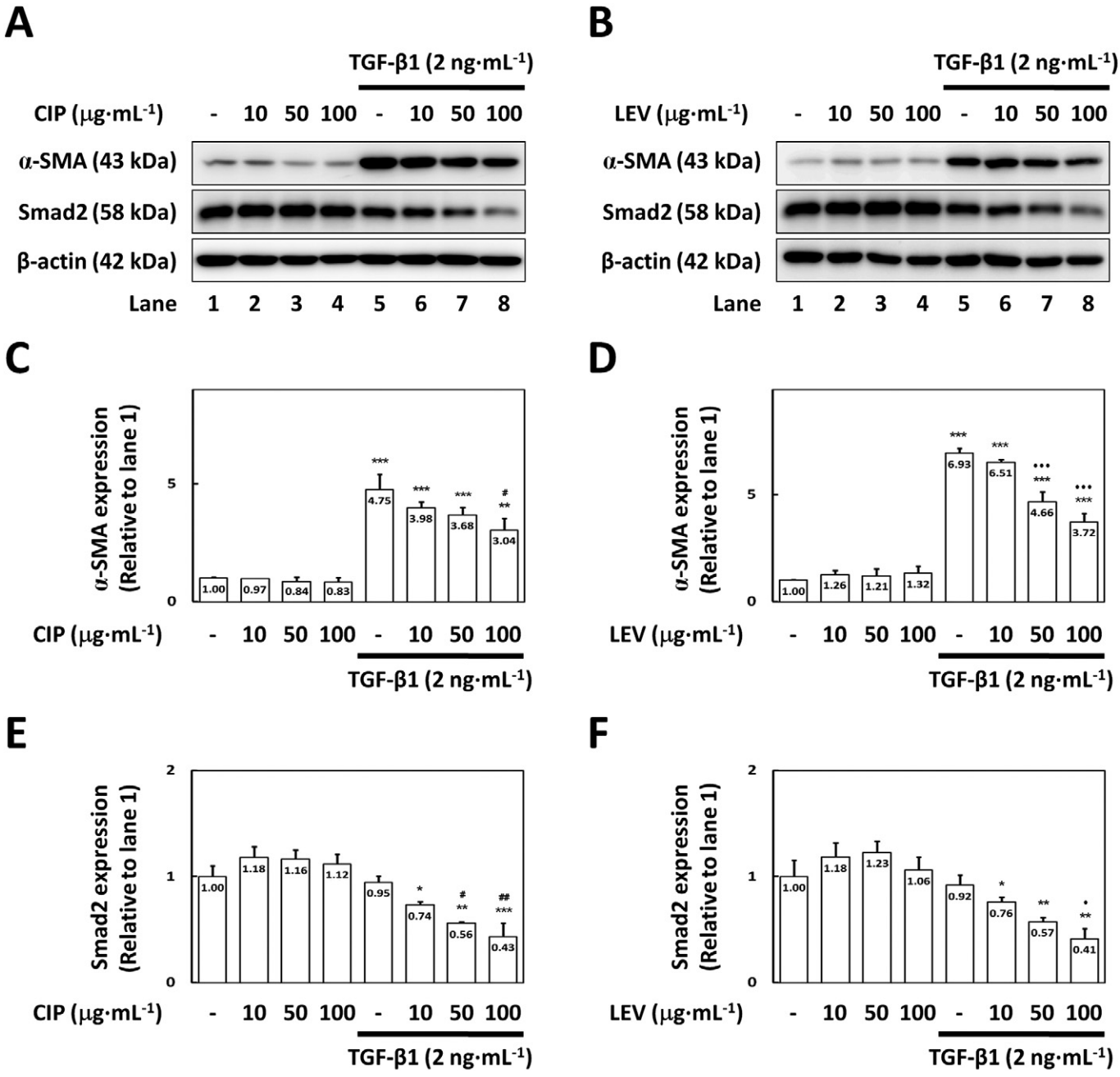

Figure 9

Effect of CIP and LEV on α-SMA and Smad2 expressions. HCFs were incubated in 2 ng·mL^{-1} TGF-β1-containing serumless DMEM with 0, 10, 50 and 100 μg·mL^{-1} of (A) CIP or (B) LEV. All the cell lysates were harvested after 3 days of incubation and analysed by immunoblotting with α-SMA-, Smad2- and β-actin-specific primary antibodies. Quantitative data were expressed as the mean ± SEM of three individual experiments performed in triplicate for (C, D) α-SMA and (E, F) Smad2 expressions respectively. Differences in the relative changes of α-SMA and Smad2 expressions were analysed by two-way ANOVA and compared with the groups in the absence of TGF-β1 (*, $P < 0.05$; **, $P < 0.01$; ***, $P < 0.001$), CIP (#, $P < 0.05$; ##, $P < 0.01$) or LEV (◆, $P < 0.05$; ◆◆◆, $P < 0.001$).

transplantation, topically frequent application of fluoroquinolones might benefit corneal ulcer treatment by minimizing corneal scar formation and by circumventing corneal transplantation.

The TGFBR1 signalling pathway is currently a potential therapeutic target for many diseases, such as breast cancer-induced osteolysis (Futakuchi *et al.*, 2009), glioblastoma (Tran *et al.*, 2007), liver cancer (Fransvea *et al.*, 2009), osteoarthritis (Blaney Davidson *et al.*, 2005), pancreatic cancer (Medicherla *et al.*, 2007) and puromycin-induced nephritis (Higashiyama *et al.*, 2007). Reported inhibitors that block the function of TGFBR1 include LY2109761 (Connolly *et al.*, 2011), SB431542 (Cabello-Verrugio *et al.*, 2011), SB525334 (Higashiyama *et al.*, 2007), SD-208

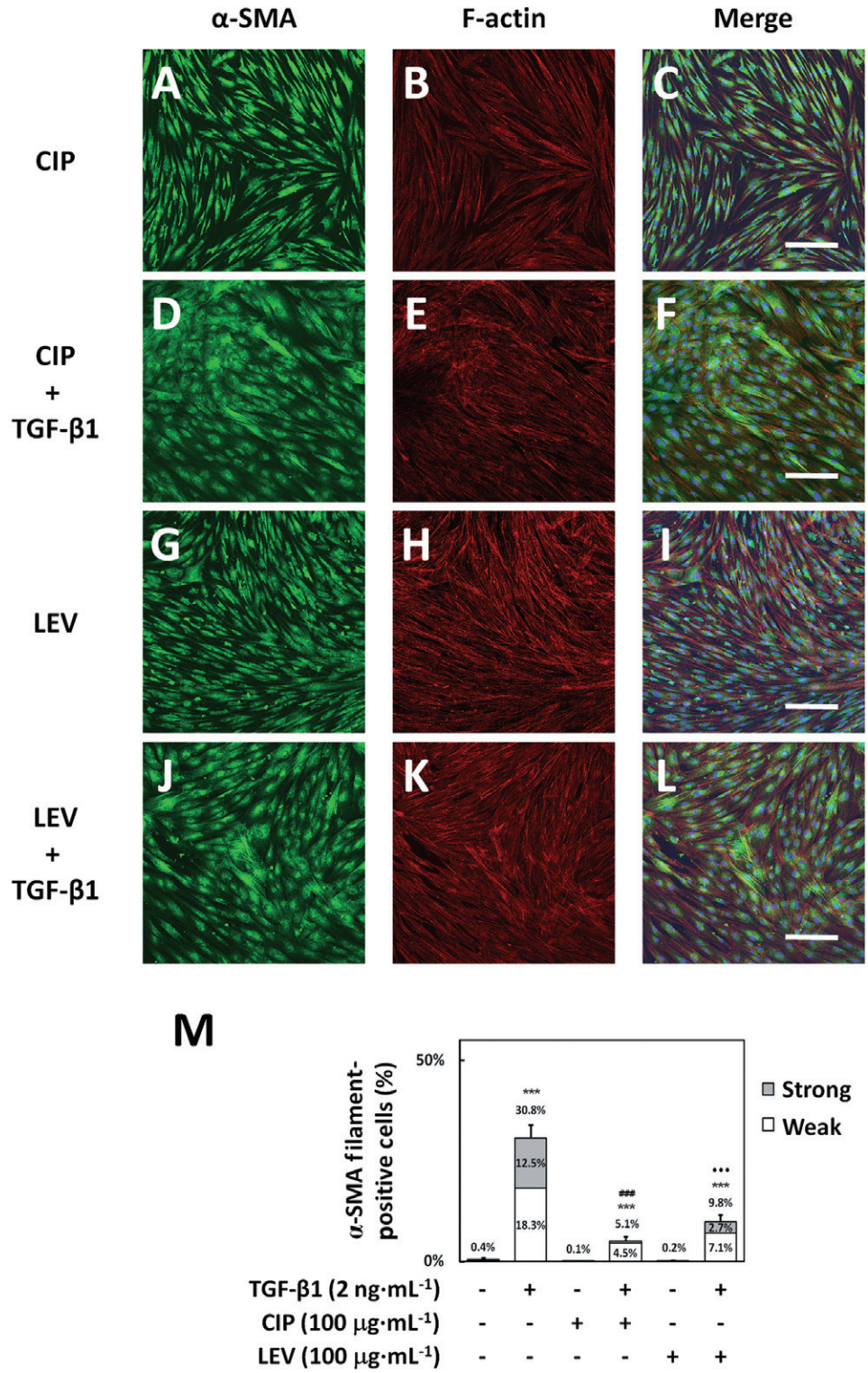

Figure 10

Suppression of α-SMA filament formation by CIP and LEV. HCFs on round cover glasses were incubated in 2 ng·mL^{-1} TGF-β1-containing serumless DMEM with 100 μg·mL^{-1} CIP or LEV for 3 days and then were stained with α-SMA-specific antibody (A, D, G, J), rhodamine phalloidin (B, E, H, K) and DAPI (shown in merged images of C, F, I, L). Scale bar in each merged image was 100 μm in length. (M) Ratio of α-SMA filament-positive HCFs was calculated from five different fields of each individual experiment at 100 × magnification. Quantitative data of the total expression ratio containing strong images (upper part of the column) and weak images (lower part of the column) were expressed as the mean ± SEM of three individual experiments performed in triplicate. Differences in the effect of CIP and LEV on α-SMA filament formation were analysed by one-way ANOVA and compared with the groups in the absence of TGF-β1 (***, $P < 0.001$), CIP (###, $P < 0.001$) or LEV (◆◆◆, $P < 0.001$).

(2,4-disubstituted pteridine) (Leung *et al.*, 2006; Medicherla *et al.*, 2007), SX-007 (Tran *et al.*, 2007) and neutralizing antibody (Futakuchi *et al.*, 2009). Even though these inhibitors have been used to suppress fibroblast-to-myofibroblast differentiation, they are not commonly used drugs in ophthalmology. In addition, targeting the TGF-β1 signalling pathway by down-regulating TGFBR2 with small interference RNAs has been reported to prevent ocular fibrosis (Nakamura *et al.*, 2004). However, application of these drugs to prevent corneal scarring has not been explored. Herein we suggest preoperative application of MOX at higher dosage as a useful alternative for reducing corneal fibrosis in corneal surgery.

DNA gyrase, a type II topoisomerase, plays important roles in a number of fundamental nuclear processes and is essential for the survival of eukaryotic cells. Quinolones inhibit the bacterial DNA gyrase thereby inhibiting DNA replication and transcription (Gruger *et al.*, 2004). Evidence has shown eukaryotic DNA gyrase as a target for a variety of quinolone-based drugs (Gruger *et al.*, 2004). Whether MOX modulates the TGFBR1 signalling via interfering with DNA gyrase awaits further study.

CIP, LEV and MOX are classified into the second-, third- and fourth-generation fluoroquinolones respectively. Both CIP and LEV kill bacteria by inhibiting DNA gyrase, but MOX inhibits both DNA gyrase and topoisomerase IV. Our results indicated that not only MOX but also CIP and LEV suppressed α-SMA protein expression (Figure 9) and α-SMA filament formation (Figure 10). However, while TGF-β1 increased α-SMA filament formation in 30.8% of treated cells, MOX, CIP and LEV at 100 $\mu g \cdot mL^{-1}$ suppressed α-SMA filament forming cells to a residual of 1.7, 5.1 and 9.8% cells forming α-SMA filaments respectively (Figures 5M and 10M). Our results suggest that MOX suppressed the α-SMA filament formation in HCFs most efficiently ($P < 0.001$).

This study is the first demonstration that MOX modulates fibroblast-to-myofibroblast differentiation of HCFs by affecting α-SMA expression in the presence of TGF-β1. Both preoperative and concomitant MOX applications may efficiently suppress corneal fibroblast-to-myofibroblast differentiation. Our novel finding of the anti-fibrotic action in addition to its original antibacterial properties provides an extension of its original application and also offers an alternative to the traditional regimen of intraoperative mitomycin C application plus post-operative MOX. As MOX treatment does not reduce pre-existing α-SMA, it should thus be used before or at least soon after wounding. Further studies investigating whether MOX triggers other regulators that modulate the inflammatory response in HCFs as shown in mitomycin C (Chang *et al.*, 2010) are warranted. Animal and/or *in vivo* studies are also needed to determine an appropriate dosage of MOX. Verifying similar anti-fibrotic effects in fibroblasts of other origins awaits further investigation and may also facilitate wound healing modulation in other tissues once validated.

Acknowledgements

This work was supported by Grant FEMH-97-C-001 from Far Eastern Memorial Hospital, Banqiao District, New Taipei City, Taiwan.

Conflict of interest

None.

References

Blaney Davidson EN, Scharstuhl A, Vitters EL, van der Kraan PM, van den Berg WB (2005). Reduced transforming growth factor-beta signaling in cartilage of old mice: role in impaired repair capacity. Arthritis Res Ther 7: R1338–R1347.

Blobe GC, Schiemann WP, Lodish HF (2000). Role of transforming growth factor beta in human disease. N Engl J Med 342: 1350–1358.

Burka JM, Bower KS, Vanroekel RC, Stutzman RD, Kuzmowych CP, Howard RS (2005). The effect of fourth-generation fluoroquinolones gatifloxacin and moxifloxacin on epithelial healing following photorefractive keratectomy. Am J Ophthalmol 140: 83–87.

Cabello-Verrugio C, Cordova G, Vial C, Zuniga LM, Brandan E (2011). Connective tissue growth factor induction by lysophosphatidic acid requires transactivation of transforming growth factor type beta receptors and the JNK pathway. Cell Signal 23: 449–457.

Chang SW (2005). Corneal keratocyte apoptosis following topical intraoperative mitomycin C in rabbits. J Refract Surg 21: 446–453.

Chang SW, Huang ZL (2006). Oral cimetidine adjuvant therapy for recalcitrant, diffuse conjunctival papillomatosis. Cornea 25: 687–690.

Chang SW, Chou SF, Chuang JL (2008a). Mechanical corneal epithelium scraping and ethanol treatment up-regulate cytokine gene expression differently in rabbit cornea. J Refract Surg 24: 150–159.

Chang SW, Chou SF, Chuang JL (2008b). Mitomycin C potentiates ultraviolet-related cytotoxicity in corneal fibroblasts. Cornea 27: 686–692.

Chang SW, Chou SF, Yu SY (2010). Dexamethasone reduces mitomycin C-related inflammatory cytokine expression without inducing further cell death in corneal fibroblasts. Wound Repair Regen 18: 59–69.

Chou SF, Chang SW, Chuang JL (2007). Mitomycin C upregulates IL-8 and MCP-1 chemokine expression via mitogen-activated protein kinases in corneal fibroblasts. Invest Ophthalmol Vis Sci 48: 2009–2016.

Chung JL, Seo KY, Yong DE, Mah FS, Kim TI, Kim EK *et al.* (2009). Antibiotic susceptibility of conjunctival bacterial isolates from refractive surgery patients. Ophthalmology 116: 1067–1074.

Connolly EC, Saunier EF, Quigley D, Luu MT, De Sapio A, Hann B *et al.* (2011). Outgrowth of drug-resistant carcinomas expressing markers of tumor aggression after long-term TbetaRI/II kinase inhibition with LY2109761. Cancer Res 71: 2339–2349.

Evans RA, Tian YC, Steadman R, Phillips AO (2003). TGF-beta1-mediated fibroblast-myofibroblast terminal differentiation – the role of Smad proteins. Exp Cell Res 282: 90–100.

Fransvea E, Mazzocca A, Antonaci S, Giannelli G (2009). Targeting transforming growth factor (TGF)-betaRI inhibits activation of beta1 integrin and blocks vascular invasion in hepatocellular carcinoma. Hepatology 49: 839–850.

Fukasawa H, Yamamoto T, Togawa A, Ohashi N, Fujigaki Y, Oda T *et al.* (2004). Down-regulation of Smad7 expression by ubiquitin-dependent degradation contributes to renal fibrosis in obstructive nephropathy in mice. Proc Natl Acad Sci U S A 101: 8687–8692.

Futakuchi M, Nannuru KC, Varney ML, Sadanandam A, Nakao K, Asai K *et al.* (2009). Transforming growth factor-beta signaling at the tumor-bone interface promotes mammary tumor growth and osteoclast activation. Cancer Sci 100: 71–81.

Gruger T, Nitiss JL, Maxwell A, Zechiedrich EL, Heisig P, Seeber S *et al.* (2004). A mutation in Escherichia coli DNA gyrase conferring quinolone resistance results in sensitivity to drugs targeting eukaryotic topoisomerase II. Antimicrob Agents Chemother 48: 4495–4504.

Higashiyama H, Yoshimoto D, Kaise T, Matsubara S, Fujiwara M, Kikkawa H *et al.* (2007). Inhibition of activin receptor-like kinase 5 attenuates bleomycin-induced pulmonary fibrosis. Exp Mol Pathol 83: 39–46.

Hindman HB, Swanton JN, Phipps RP, Sime PJ, Huxlin KR (2010). Differences in the TGF-{beta}1-induced profibrotic response of anterior and posterior corneal keratocytes in vitro. Invest Ophthalmol Vis Sci 51: 1935–1942.

Hinz B, Phan SH, Thannickal VJ, Galli A, Bochaton-Piallat ML, Gabbiani G (2007). The myofibroblast: one function, multiple origins. Am J Pathol 170: 1807–1816.

Holland EJ, Lane SS, Kim T, Raizman M, Dunn S (2008). Ocular penetration and pharmacokinetics of topical gatifloxacin 0.3% and moxifloxacin 0.5% ophthalmic solutions after keratoplasty. Cornea 27: 314–319.

Huet E, Vallee B, Szul D, Verrecchia F, Mourah S, Jester JV *et al.* (2008). Extracellular matrix metalloproteinase inducer/CD147 promotes myofibroblast differentiation by inducing alpha-smooth muscle actin expression and collagen gel contraction: implications in tissue remodeling. FASEB J 22: 1144–1154.

Hutcheon AE, Guo XQ, Stepp MA, Simon KJ, Weinreb PH, Violette SM *et al.* (2005). Effect of wound type on Smad 2 and 4 translocation. Invest Ophthalmol Vis Sci 46: 2362–2368.

Isenberg JI, Peterson WL, Elashoff JD, Sandersfeld MA, Reedy TJ, Ippoliti AF *et al.* (1983). Healing of benign gastric ulcer with low-dose antacid or cimetidine. A double-blind, randomized, placebo-controlled trial. N Engl J Med 308: 1319–1324.

Kaji Y, Soya K, Amano S, Oshika T, Yamashita H (2001). Relation between corneal haze and transforming growth factor-beta1 after photorefractive keratectomy and laser in situ keratomileusis. J Cataract Refract Surg 27: 1840–1846.

Kato M, Arce L, Wang M, Putta S, Lanting L, Natarajan R (2011). A microRNA circuit mediates transforming growth factor-beta1 autoregulation in renal glomerular mesangial cells. Kidney Int 80: 358–368.

Katz HR, Masket S, Lane SS, Sall K, Orr SC, Faulkner RD *et al.* (2005). Absorption of topical moxifloxacin ophthalmic solution into human aqueous humor. Cornea 24: 955–958.

Kernt M, Neubauer AS, Liegl RG, Lackerbauer CA, Eibl KH, Alge CS *et al.* (2009). Intracameral moxifloxacin: in vitro safety on human ocular cells. Cornea 28: 553–561.

Leung SY, Niimi A, Noble A, Oates T, Williams AS, Medicherla S *et al.* (2006). Effect of transforming growth factor-beta receptor I kinase inhibitor 2,4-disubstituted pteridine (SD-208) in chronic allergic airway inflammation and remodeling. J Pharmacol Exp Ther 319: 586–594.

Lindstrom R, Lane S, Cottingham A, Smith S, Sall K, Silverstein S *et al.* (2010). Conjunctival concentrations of a new ophthalmic solution formulation of moxifloxacin 0.5% in cataract surgery patients. J Ocul Pharmacol Ther 26: 591–595.

Maltseva O, Folger P, Zekaria D, Petridou S, Masur SK (2001). Fibroblast growth factor reversal of the corneal myofibroblast phenotype. Invest Ophthalmol Vis Sci 42: 2490–2495.

Matsuzaki K (2011). Smad phosphoisoform signaling specificity: the right place at the right time. Carcinogenesis 32: 1578–1588.

Medicherla S, Li L, Ma JY, Kapoun AM, Gaspar NJ, Liu YW *et al.* (2007). Antitumor activity of TGF-beta inhibitor is dependent on the microenvironment. Anticancer Res 27: 4149–4157.

Nakamura H, Siddiqui SS, Shen X, Malik AB, Pulido JS, Kumar NM *et al.* (2004). RNA interference targeting transforming growth factor-beta type II receptor suppresses ocular inflammation and fibrosis. Mol Vis 10: 703–711.

Netto MV, Mohan RR, Ambrosio R, Jr, Hutcheon AE, Zieske JD, Wilson SE (2005). Wound healing in the cornea: a review of refractive surgery complications and new prospects for therapy. Cornea 24: 509–522.

Pannu J, Nakerakanti S, Smith E, ten Dijke P, Trojanowska M (2007). Transforming growth factor-beta receptor type I-dependent fibrogenic gene program is mediated via activation of Smad1 and ERK1/2 pathways. J Biol Chem 282: 10405–10413.

Pestova E, Millichap JJ, Noskin GA, Peterson LR (2000). Intracellular targets of moxifloxacin: a comparison with other fluoroquinolones. J Antimicrob Chemother 45: 583–590.

Petridou S, Maltseva O, Spanakis S, Masur SK (2000). TGF-beta receptor expression and smad2 localization are cell density dependent in fibroblasts. Invest Ophthalmol Vis Sci 41: 89–95.

Saika S, Ikeda K, Yamanaka O, Flanders KC, Okada Y, Miyamoto T *et al.* (2006). Loss of tumor necrosis factor alpha potentiates transforming growth factor beta-mediated pathogenic tissue response during wound healing. Am J Pathol 168: 1848–1860.

Saika S, Yamanaka O, Sumioka T, Miyamoto T, Miyazaki K, Okada Y *et al.* (2008). Fibrotic disorders in the eye: targets of gene therapy. Prog Retin Eye Res 27: 177–196.

Tandon A, Tovey JC, Sharma A, Gupta R, Mohan RR (2010). Role of transforming growth factor beta in corneal function, biology and pathology. Curr Mol Med 10: 565–578.

Tang Y, Urs S, Boucher J, Bernaiche T, Venkatesh D, Spicer DB *et al.* (2010). Notch and transforming growth factor-beta (TGFbeta) signaling pathways cooperatively regulate vascular smooth muscle cell differentiation. J Biol Chem 285: 17556–17563.

Tran TT, Uhl M, Ma JY, Janssen L, Sriram V, Aulwurm S *et al.* (2007). Inhibiting TGF-beta signaling restores immune surveillance in the SMA-560 glioma model. Neuro Oncol 9: 259–270.

Webber J, Meran S, Steadman R, Phillips A (2009). Hyaluronan orchestrates transforming growth factor-beta1-dependent maintenance of myofibroblast phenotype. J Biol Chem 284: 9083–9092.

Yasueda S, Higashiyama M, Yamaguchi M, Isowaki A, Ohtori A (2007). Corneal critical barrier against the penetration of dexamethasone and lomefloxacin hydrochloride: evaluation by the activation energy for drug partition and diffusion in cornea. Drug Dev Ind Pharm 33: 805–811.

Yoshida J, Kim A, Pratzer KA, Stark WJ (2010). Aqueous penetration of moxifloxacin 0.5% ophthalmic solution and besifloxacin 0.6% ophthalmic suspension in cataract surgery patients. J Cataract Refract Surg 36: 1499–1502.